

**Identification of Turbostratic Twisting in Germanene**

Journal:	<i>Journal of Materials Chemistry C</i>
Manuscript ID	TC-ART-04-2019-002064.R2
Article Type:	Paper
Date Submitted by the Author:	10-Jul-2019
Complete List of Authors:	Trout, Amanda; Ohio State University, Materials Science and Engineering Wang, Yaxian; Ohio State University, Materials Science and Engineering Esser, Bryan; Ohio State University, Materials Science and Engineering Jiang, Shishi; The Ohio State University, Chemistry and Biochemistry Goldberger, Joshua; The Ohio State University, Chemistry Windl, Wolfgang; Ohio State University, Materials Science and Engineering McComb, David; The Ohio State University,

ARTICLE

Identification of Turbostratic Twisting in Germanane

Amanda H. Trout,^{a,b} Yaxian Wang,^b Bryan D. Esser,^a Shishi Jiang,^c Joshua E. Goldberger,^c Wolfgang Windl,^b and David W. McComb^{a,b*}

Received 00th January 20xx,
Accepted 00th January 20xx

DOI: 10.1039/x0xx00000x

Germanane, a van der Waals layered material predicted to have a direct band gap and high carrier mobility, is a promising two-dimensional material with applications in optoelectronics. The electronic properties of germanane have been well studied; however, experimentally measured properties are orders of magnitude lower than predicted values, potentially limiting the future device applications. The structure of germanane contains an inherent disorder along the *c*-axis, resulting in a diffuse halo with hexagonal symmetry in the electron diffraction pattern. The origin of this disorder is not well understood, further limiting the device application of germanane. Here, we have used experimental and simulated electron diffraction patterns to show that this diffuse scattering arises from turbostratic disorder present in the germanane structure with rotational disorder as the main contribution. The maximum rotation angle in the examined germanane crystal is limited to three degrees. For larger angles, germanane would become unstable as DFT calculations show. DFT calculations also indicate that small angle rotations cause a change in charge distribution in Ge and H atoms, and thus should affect the electronic properties of germanane considerably. This study explains for the first time the origin of the *c*-axis disorder in this van der Waals structure and establishes computationally analyzed diffraction patterns as a tool to quantify turbostratic disorder.

Introduction

Since the discovery of single layer graphene in 2004,^{1,2} there has been an increase in the development of new van der Waals layered materials that can be easily exfoliated to single or few monolayers.³⁻⁶ The properties and electronic structure of these materials can be tuned *via* chemical functionalization, providing numerous opportunities for novel applications and devices.⁶⁻⁹ One such material, germanane (GeH), is a germanium analog of graphene (CH). Each layer of GeH consists of sp³-hybridized Ge atoms bonded to three Ge atoms in-plane in a honeycomb arrangement and a H atom out-of-plane. GeH has been shown to have a direct bandgap of 1.56 eV and predicted to have 5× higher electron mobilities compared to bulk Ge.^{9,10} Additionally, this material has garnered research interest as its electronic structure can be tuned by replacing the H atom with various ligands.^{8,9} Although germanane is promising for electronic and optoelectronic applications, its observed electronic transport behavior is well below predicted values.¹¹⁻¹³ A possible cause could be disorder along the *c*-axis which has been previously observed by X-ray diffraction, although the exact nature has not

been determined to date.⁹ Possibilities include translational (which includes stacking faults) and rotational disorder. The latter has been observed in other van der Waals layered materials, such as graphite, where it is called turbostratic disorder.¹⁴⁻¹⁷ If the turbostratic disorder introduced changes the electron distribution in neighboring layers, these changes would scatter electrons,¹⁸ increase the electrical resistivity, and thus be a cause for the unexpectedly low conductivity. On the other hand, if few-layer flakes with twisted sheets are exfoliated, germanane and other graphene analogues could show novel electronic properties of similarly unexpected nature, as the recently predicted localized Dirac electrons in twisted bilayer graphene¹⁹ and thus open new possibilities in the emerging field of twistronics.^{20,21} In the following, we will show that the disorder observed in germanane is indeed of turbostratic nature and explore the limits of possible rotational angles as well as its effect on the electronic properties.

While turbostratic disorder in graphite has been studied *via* Raman spectroscopy and broadening in X-ray diffraction powder patterns, turbostratic disorder in germanane has not yet been investigated.^{15,16,22-25} The previously reported synchrotron X-ray powder diffraction of GeH does show significantly broadened diffraction reflections,²⁶ however, it is incredibly difficult to unambiguously differentiate if this peak broadening is a consequence of smaller domain sizes, stacking faults, or rotational, translational, and curvature between layers.²² Other techniques are needed to further identify and understand turbostratic disorder in van der Waals layered

^a Center for Electron Microscopy and Analysis, The Ohio State University, Columbus, Ohio 43210, USA.

^b Department of Materials Science and Engineering, The Ohio State University, Columbus, Ohio 43210, USA.

^c Department of Chemistry and Biochemistry, The Ohio State University, 151 W Woodruff Ave, Columbus, 43210 Ohio, USA.

* Email: mccomb.29@osu.edu

† Electronic Supplementary Information (ESI) available: DFT results and figures for translated GeH layers and Bader charges on Ge and H in turbostratic GeH. See DOI: 10.1039/x0xx00000x

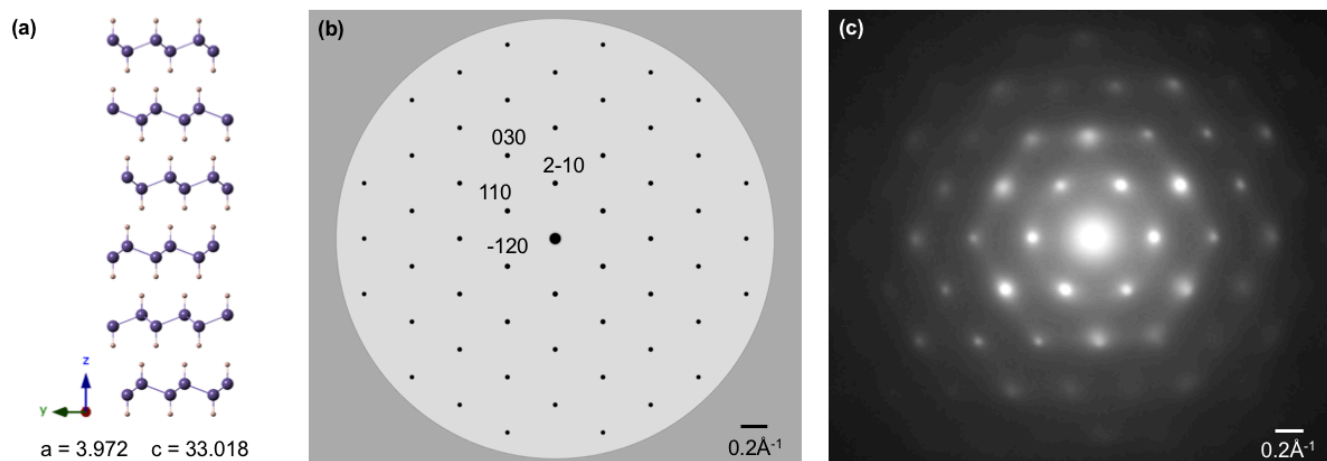


Figure 1: (a) [1 0 0] view of perfect structure 6R GeH highlighting the AA'BB'CC' stacking (purple: Ge; pink: H) (b) Simulated diffraction pattern of single crystal GeH. (c) Experimental diffraction pattern of GeH containing a diffuse hexagonal halo.

materials. Transmission electron microscopy (TEM) is one of the most powerful and heavily used techniques for the structural analysis of materials and is well suited for single and multiple-layer thick 2D materials.^{3,6} Here we have used selected area electron diffraction (SAED) in the TEM, combined with inelastic-scattering based diffraction simulations and density functional theory (DFT) calculations to study turbostratic disorder in germanane and its effects on the electronic properties. We also show that this combination provides a powerful new approach for determining rotation angles in turbostratically disordered systems and enables new characterization capabilities for twisted van der Waals systems.

Experimental section

Synthesis and Characterization

GeH was synthesized by deintercalation of the Zintl phase β -CaGe₂ in HCl as previously reported.²⁶ Bulk GeH flakes were ground using a mortar and pestle, and Cu lacey carbon grids were rubbed over the ground material resulting in flakes with a range of thicknesses, some only two to three layers thick, dispersed on the grid. TEM images and electron diffraction patterns were collected using a FEI/Philips CM-200T TEM operating at 200 kV. Each diffraction pattern was collected using a 40 or 10 micron selected area aperture and an exposure of 0.5 second.

DFT Calculations

Density functional theory (DFT) calculations were performed using the Vienna *ab initio* Simulation Package (VASP)^{27,28} within the generalized gradient approximation (GGA) with Perdew-Burke-Ernzerhof (PBE)²⁹ functional and a plane-wave cut-off of 250 eV and Γ point integration in reciprocal space.³⁰ To simulate the random rotation between adjacent layers in bulk GeH, we have used periodic 2H-GeH structures along the *c*-axis with isolated disk shape sheets along the *a/b*-axis. The edges of the disc stack in the *a/b*-plane are separated by at least 10 Å in all radial directions to minimize interactions.

After rotation, the Ge atoms are kept fixed to simulate the constraints of near-bulk size, while the H atoms are fully relaxed until the forces on all atoms are less than 10⁻⁴ eV/Å. The stability for each structure is evaluated by the adhesion energy per Ge atom, defined as the energy change when the GeH layers are pulled apart. Convergence tests showed that the adhesion energy converges to ~0.5 meV per Ge atom for 10 Å separation, which then was used for all calculations.

Results and Discussion

GeH has a rhombohedral unit cell of space group $R\bar{3}m$ with $a = 3.972$ Å and $c = 33.018$ Å with 6-layers per unit cell,²⁶ as shown in Figure 1a and confirmed using SAED. The reflections in the experimental diffraction pattern were measured to be within 5% of theoretical values (Figure 1c). SAED was also used to probe the quality of the material. Perfect, single crystals exhibit sharp, symmetric Bragg reflections as expected by the calculated diffraction pattern for GeH generated using CrystalDiffract[®] in Figure 1b.³¹ The experimental electron diffraction pattern of GeH exhibits sharp Bragg reflections, as well as a diffuse “hexagonal” halo. Typically in electron diffraction, diffuse halos are circularly symmetric forming rings or diffuse arcs between diffraction reflections. Here, however, intensity profiles (Figure S1) indicate sharp lines of diffuse intensity between reflections giving rise to halos that are hexagonally symmetric. Diffuse halos and blurring between electron diffraction reflections can be observed for a variety of reasons, e.g. roughness/curvature of the specimen, phonons, beam damage, disorder, *etc.* Therefore, a number of experiments were conducted to identify the source of the halo in this system.

A low temperature experiment using a cryogenic TEM specimen holder was performed to determine whether the hexagonal halo was caused by directional phonon vibrations. However, there was no change in the diffraction pattern collected at 80 K (Figure 2c) compared with room temperature (Figure 2b). Electron beam induced damage by radiolysis or knock-on mechanisms can lead to amorphization of the crystal

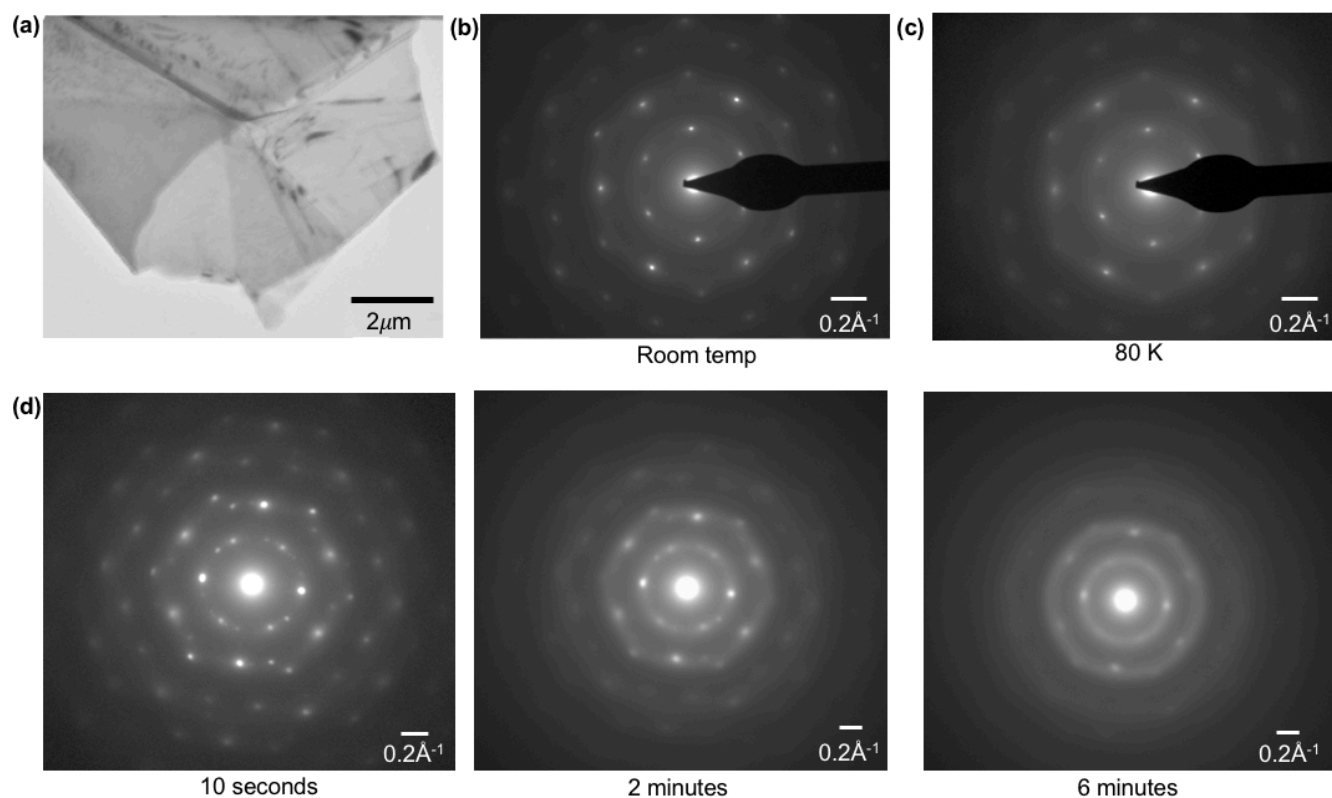


Figure 2: (a) Bright field TEM image of GeH flake. Experimental diffraction patterns collected at (b) room temperature and (c) 80 K (right). (d) Experimental diffraction patterns showing the progression of beam damage over time after initial exposure.

structure, which can result in diffuse halos in the electron diffraction pattern. This possibility was investigated by carrying out a dose-controlled experiment where the exposure of the germanane flakes to the electron beam was minimized during set-up, a diffraction pattern was formed using a low electron dose and the diffraction pattern was monitored as a function of total accumulated electron dose. The series of images in Figure 2c, show diffraction patterns for the same particle after beam exposure. Electron beam damage results in gradual fading of the Bragg diffraction maxima and the transition of the hexagonal halo to a more diffuse circular halo associated with amorphous material is observed. Based on these observations the hexagonal halo is neither attributed to phonons nor electron beam damage.

It has been well established that 2D materials in the few layer limit are typically not flat but corrugated.^{32,33} The bright field TEM image in Figure 2(a) shows a GeH flake with multiple layers containing ripples, wrinkles, and/or folds, and as a consequence, the electron diffraction pattern of GeH contains blurred and broadened reflections. This affect alone however could not cause diffuse halos of hexagonal symmetry, as it has been shown that the rough nature of the specimen causes the electron diffraction reflections to broaden concentrically.^{32,33} Since the hexagonal symmetry would be compatible with the assumptions that a range of interplanar spacings are diffracted with some rotational disorder, we hypothesize that the electron diffraction provides evidence for the presence of turbostratic disorder in germanane. While graphite can accommodate a wide range of rotations, lattice rotations in germanane are restricted due to the hydrogen atoms between each layer that

create significant steric hinderance for larger rotation angles. However, it was initially unclear what range of rotation angles would be energetically acceptable. Additionally, it was not clear if translational disorder in addition to rotations would be important or not. In order to answer these questions, we performed DFT calculations of the energetics of rotations and translations in crystalline germanane with 2H structure.

The stability of random rotations between adjacent GeH layers was evaluated for three different lateral domain sizes of GeH disks, with diameters 1.6 nm (Figure 3c), 2.55 nm and 3.2 nm (Figure 3b). The average crystalline domain size in GeH can vary depending on the synthesis method, and has been reported to range from 2.8 to 17.6 nm, with a mean value of ~10 nm.²⁸ The adhesion energy per Ge atom is calculated at different rotation angles, as shown in Figure 3a. For all disk sizes, the adhesion energy drops with increasing rotation angle, indicating a decrease of stability with increasing turbostratic disorder. Moreover, adhesion energy at zero rotation increases with sheet diameter, and for very large sheets would approach that of the bulk (red solid square). Due to the steric interaction of H atoms in neighboring rows (Figures 3c,4a), however, adhesion energy decreases noticeably faster for larger sheets than smaller ones. In larger sheets, hydrogen atoms experience steric hindrance at a much smaller angle, which significantly raises the energy penalty. The largest sheet examined has negative adhesion energy with a ~7.5° rotation (Figure 3a), after which the van der Waals structure will decompose instead of rotating further. For real samples having domain sizes that are easily tens of nanometers, the maximum rotation angle (γ) is expected to be much smaller. The geometric correlation

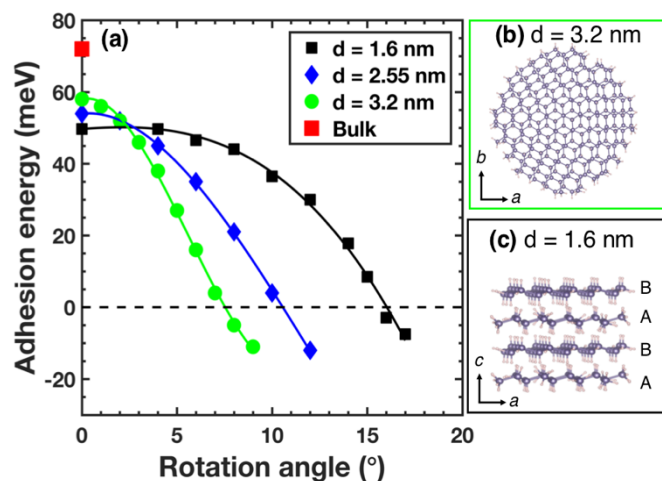


Figure 3: (a). Adhesion energy per Ge atom with respect to rotation angle calculated in a 2H structure by DFT. (b-c). Sheets only with smallest (1.6 nm, black, highlighting the steric interaction between H atoms) and largest (3.2 nm, green, highlighting the disk shape of the simulated system) diameters are shown for clarity. Stability of GeH structure with turbostratic disorder decreases with rotation; and it is more evident in larger sheets.

between grain size and maximum rotation angle is demonstrated in Figure 4a.

The distance between two neighboring H rows, denoted as d , is 3.99 Å. At a small rotation angle limit and sufficiently large disk diameter D , γ can be written as $\gamma \approx \sin \gamma = d/D$. The reciprocal correlation between γ and D is plotted in Figure 4b. Since, as described above, the average domain size for experimental GeH flakes is on the order of $D \sim 10$ nm,³⁴ the extrapolated rotation angle for turbostratic disorder in an experimentally grown crystal should be limited to 3 degrees.

In order to confirm that turbostratic disorder is the source of the hexagonal halo in the experimental diffraction patterns for GeH, electron diffraction patterns were simulated. A structure with rotations $-3^\circ \leq \gamma \leq 3^\circ$ was created using a MATLAB script[†]. Starting with a perfect unit cell in which the Ge atoms are in the chair conformation (Figure 1a), the height of

the Ge atoms in each layer was averaged along the c -axis to create six flat layers per unit cell. To take into account the possibility of distortion in the buckled honeycomb framework, the magnitude of thermal vibration of Ge atoms was verified by phonon calculations, with a mean square displacement of 0.05 Å². The displacements were restricted to the three Ge-Ge bonding directions, due to steric hindrance from the H atoms on each Ge. Each layer in the unit cell was rotated *via* a rotation matrix that randomly assigns an angle of rotation within a specified range of $\pm 3^\circ$.

The TEM diffraction pattern for this structure was simulated using μ STEM, a software package used to simulate various imaging modes for both scanning and conventional TEM based on inelastic scattering.³⁵ The quantum excitation of phonons mode was used with GeH specimen thickness of 132 Å along the beam direction and one projected potential per monolayer of GeH. The simulated diffraction pattern, Figure 4c, shows additional Bragg reflections that form small linear segments causing the appearance of a hexagonal halo. The hexagonal halo becomes more prominent further away from the zero-order beam, consistent with the experimental diffraction patterns.

Turbostratic disorder consists of random translations in addition to rotations. To determine the influence of translational effects, the potential energy of planar translations between two perfect buckled honeycomb GeH layers was calculated by DFT. As expected, a contour plot shows that translations are not energetically favorable. The energy barrier for translating a lattice vector along a/b axis can be as high as 10 meV/Ge atom in bulk structures (see supplemental Figure S1). Additionally, the simulated diffraction pattern containing only translations does not show the hexagonal halo (Figure S2c). Therefore, pure translational disorder between neighboring GeH layers cannot be the direct cause for the diffuse halo.

Finally, we investigate the electronic properties of turbostratic GeH by density functional theory. Since the small simulation disks we are using, which lack periodic boundary conditions, do not allow for meaningful band structure calculations, we performed a Bader charge analysis³⁶ for 3.2 nm

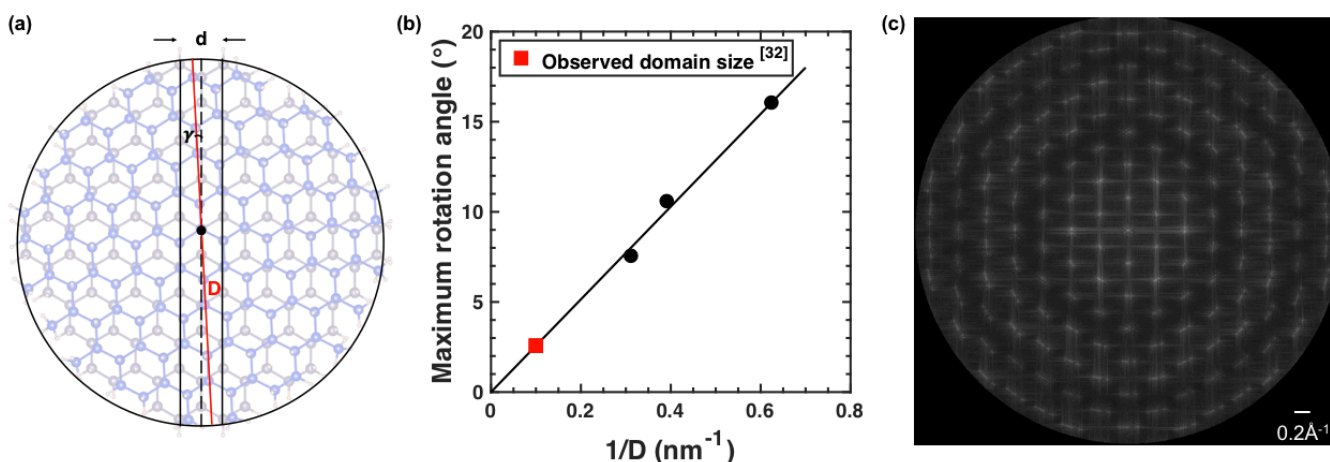


Figure 4: (a) Geometric representation of relationship between rotation angle (γ), disk diameter (D) and distance between neighboring hydrogen rows (d). Atomic structure with 3° rotation for the largest disk simulated is highlighted by different colors of Ge atoms. (b) Extrapolated maximum rotation angle (red square) for an observed grain with D10 nm shows a 3° rotation between GeH layers causes the diffusion halo. (c) Simulated electron diffraction pattern of GeH structure containing random rotations of $\pm 3^\circ$

disc size to determine the charges on Ge and H atoms as a function of rotation. Histograms of the respective charge distributions for rotation angles of 0°, 3°, and 5° are shown in Figure S3, along with the average charges. To eliminate the effect of the edge atoms, we only evaluate Ge/H atoms within a radius of 0.5 to 1.5 nm around the disc center. Our results show that even small rotations result in charge transfer shifts between Ge and H atoms. Whereas for untwisted germanane, the Bader analysis suggests a transfer of ~0.3 electrons from Ge to H on average, similar to the bulk value, this transfer decreases with rotation. Even though our simulated discs are limited by computational constraints to highly un-bulk-like sizes with a rather broad initial Bader charge distribution compared to the sharp bulk value, these results show that even small rotations cause a significant redistribution of charges, and thus a significant distribution of electronic scattering centers, which can be expected to significantly increase the electrical resistivity.¹⁸ A qualitative examination of the energy gap in the 3.2 nm disk shows a ~ 0.2 eV increase compared to the bulk 2H GeH structure (Figure S4). Furthermore, small rotation angles up to 5° do not have a significant effect on the gap size, which indicates that our disks with full edge passivation have a “clean” band gap and thus no edge states. Therefore, electron scattering from mid-gap states is not expected to be prevalent in the twisted GeH bilayers. While a quantitative evaluation of the magnitude is outside the scope of this paper, it is highly conceivable that this very large concentration of scattering centers (basically every atom in the structure), even if all atoms have only moderately changed charges, has a very large effect on conductivity measurements of the order of magnitude observed in experiments.

Conclusions

In conclusion, we have identified the presence of turbostratic disorder in van der Waals layered germanane based on the presence of diffuse hexagonal halos in its electron diffraction patterns. The presence of this halo at both room temperature and at 80 K rules out lattice vibrations as the source of this halo. Furthermore, beam damage induced amorphization results in circular halos. To fully understand the source of the turbostratic disorder in germanane, we investigated thermal stability of GeH disks with different sizes under translation and different rotation angles using density functional theory (DFT). We show that the rotation angle is limited to $\pm 3^\circ$ before decomposition of the GeH van der Waals layers. Simulation of diffraction patterns confirms that a small rotational disorder of $\pm 3^\circ$ between layers are enough to reproduce the hexagonal halos. Overall, our experiments and simulations establish the experimental signatures for the small turbostratic disorder in layered materials when using electron diffraction patterns. Other than in graphene where the interlayer interactions are weaker, twisted layers in germanane cause stronger shifts in the local charges on the atoms due to the steric interaction between the H atoms upon rotation. Since the charge changes affect all atoms in the rotated layers, we argue that turbostratic disorder is a plausible cause for the

experimentally observed unexpectedly high electrical resistivity in germanane. It would still be interesting to examine the bulk-like band structure of few-layer twisted germanane with a model Hamiltonian similar to previous work³⁷ or bilayer graphene to see if “magic angles” with unexpected electronic properties exist, since angles of 1.1° (found to be magic for graphene) would still be in the stability range for small enough flakes.²¹ The method of identifying rotational disorder in layered materials introduced here may help to pave the way for the further study and development of the electronic properties in twisted germanane and analogous materials.

Acknowledgements

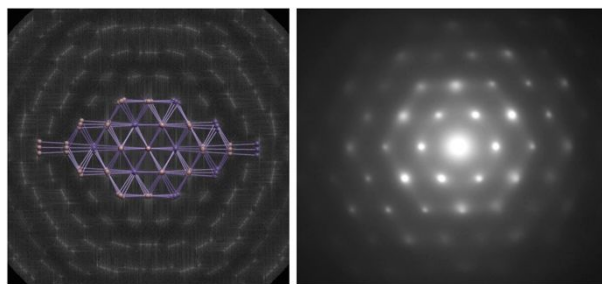
This work was supported by the Center for Emergent Materials, an NSF-funded MRSEC under Award No. DMR-1420451.

Notes and references

‡ MATLAB script used to create GeH structures with rotated layers is available upon request.

- 1 K. S. Novoselov, A. K. Geim, S. V. Morozov, D. Jiang, Y. Zhang, S. V. Dubonos, I. V. Grigorieva, and A. A. Firsov, *Science* **306**, 666–669 (2004).
- 2 K. S. Novoselov, D. Jiang, F. Schedin, T. J. Booth, V. V. Khotkevich, S. V. Morozov, A. K. Geim, and T. Maurice Rice, *Proc. Natl. Acad. Sci. U. S. A.* **102**, 10451–10453 (2005).
- 3 D. S. Schulman, A. J. Arnold, A. Razavieh, J. Nasr, and S. Das, *IEEE Nanotech. Mag.* **11**, 6–17 (2017).
- 4 R. Lv, J. A. Robinson, R. E. Schaak, D. Sun, Y. Sun, T. E. Mallouk, and M. Terrones, *Acc. Chem. Res.* **48**, 56–64 (2015).
- 5 H. Wang, F. Liu, W. Fu, Z. Fang, W. Zhou, and Z. Liu, *Nanoscale* **6**, 12250–12272 (2014).
- 6 S. Z. Butler, S. M. Hollen, L. Cao, Y. Cui, J. A. Gupta, H. R. Gutierrez, T. F. Heinz, S. Sae Hong, J. Huang, A. F. Ismach, E. Johnston-Halperin, M. Kuno, V. V. Plashnitsa, R. D. Robinson, R. S. Ruoff, S. Salahuddin, J. Shan, L. Shi, M. G. Spencer, M. Terrones, W. Windl, and J. E. Goldberger, *ACS Nano* **7**, 2898–2926 (2013).
- 7 T. Li, and J. E. Goldberger, *Chem. Mater.* **27**, 3549–3559 (2015).
- 8 S. Jiang, M. Q. Arguilla, N. D. Cultrara, and J. E. Goldberger, *Acc. Chem. Res.* **48**, 144–151 (2015).
- 9 E. Bianco, S. Butler, S. Jiang, O. D. Restrepo, W. Windl, and J. E. Goldberger, *ACS Nano* **7**, 4414–4421 (2013).
- 10 W. Amamou, P. M. Odenthal, E. J. Bushong, D. J. O’Hara, Y. Kelly Luo, J. van Baren, I. Pinchuk, Y. Wu, A. S. Ahmed, J. Katoch, M. W. Bockrath, H. W. K. Tom, J. E. Goldberger, and R. K. Kawakami, *2D Mater.* **2**, 35012 (2015).
- 11 B. N. Madhushankar, A. Kaverzin, T. Giousis, G. Potsi, D. Gournis, P. Rudolf, G. R. Blake, C. H. van der Wal, and B. J. van Wees, *2D Mater.* **4**, 21009 (2017).
- 12 J. R. Young, B. Chitara, N. D. Cultrara, M. Q. Arguilla, S. Jiang, F. Fan, E. Johnston-Halperin, and J. E. Goldberger, *J. Phys.: Condens. Matter* **28**, 34001 (2016).
- 13 N. D. Cultrara, M. Q. Arguilla, S. Jiang, C. Sun, M. R. Scudder, R. Dominic Ross, and J. E. Goldberger, *Beilstein J. Nanotechnol.* **8**, 1642–1648 (2017).
- 14 G. Vogg, M. S. Brandt, and M. Stutzmann, *Adv. Mater.*, **12**, 17 (2000).
- 15 D. Weber, L. M. Schoop, V. Duppel, J. M. Lippmann, J. Nuss, and B. V. Lotsch, *Nano Lett.* **16**, 3578–3584 (2016).

- 16 A. Wollbrink, K. Volgmann, J. Koch, K. Kanthasamy, C. Tegenkamp, Y. Li, H. Richter, S. Kamnitz, F. Steinbach, A. Feldhoff, and J. Caro, *Carbon* **106**, 93–105 (2016).
- 17 M. M. Smeller, C. L. Heideman, Q. Lin, M. Beekman, M. D. Anderson, P. Zschack, I. M. Anderson, and D. C. Johnson, *Z. Anorg. Allg. Chem.* **638**, 2632–2639 (2012).
- 18 C. Wei, N. Antolin, O. D. Restrepo, W. Windl, and J. C. Zhao, *Acta Mater.* **126**, 272–279 (2017).
- 19 G. Trambly de Laissardière, D. Mayou, and L. Magaud, *Nano Lett.* **10**, 804–808 (2010).
- 20 Y. Cao, V. Fatemi, S. Fang, K. Watanabe, T. Taniguchi, E. Kaxiras, and P. Jarillo-Herrero, *Nature* **556**, 43–50 (2018).
- 21 Y. Cao, V. Fatemi, A. Demir, S. Fang, S. L. Tomarken, J. Y. Luo, J. D. Sanchez-Yamagishi, K. Watanabe, T. Taniguchi, E. Kaxiras, R. C. Ashoori, and P. Jarillo-Herrero, *Nature* **556**, 80–84 (2018).
- 22 Z. Q. Li, C. J. Lu, Z. P. Xia, Y. Zhou, and Z. Luo, *Carbon* **45**, 1686–1695 (2007).
- 23 J. A. Garlow, L. K. Barrett, L. Wu, K. Kisslinger, Y. Zhu, and J. F. Pulecio, *Sci. Rep.* **6**, (2016).
- 24 P. Parent, C. Laffon, I. Marhaba, D. Ferry, T. Z. Regier, I. K. Ortega, B. Chazallon, Y. Carpentier, and C. Focsa, *Carbon* **101**, 86–100 (2016).
- 25 W. Fang, A. L. Hsu, R. Caudillo, Y. Song, A. Glen Birdwell, E. Zakar, M. Kalbac, M. Dubey, T. Palacios, M. S. Dresselhaus, P. T. Araujo, and J. Kong, *Nano Lett.* **13**, 1541–1548 (2013).
- 26 N. D. Cultrara, Y. Wang, M. Q. Arguilla, M. R. Scudder, S. Jiang, W. Windl, and J. E. Goldberger, *Chem. Mater.* **30**, 1335–1343 (2018).
- 27 G. Kresse, and J. Hafner, *Phys. Rev. B* **47**, 558 (1993).
- 28 G. Kresse, and J. Hafner, *Phys. Rev. B* **49**, 14251 (1994).
- 29 J. P. Perdew, K. Burke, and M. Ernzerhof, *Phys. Rev. Lett.* **77**, 3865 (1996).
- 30 G. Kresse, and J. Furthmüller, *Phys. Rev. B* **54**, 11169 (1996).
- 31 CrystalMaker Software Ltd, Oxford, England. www.crystallmaker.com
- 32 J. C. Meyer, A. K. Geim, M. I. Katsnelson, K. S. Novoselov, D. Obergfell, S. Roth, C. Girit, and A. Zettl, *Solid State Commun.* **143**, 101–109 (2007).
- 33 J. C. Meyer, A. K. Geim, M. I. Katsnelson, K. S. Novoselov, T. J. Booth, and S. Roth, *Nature* **446**, 60–63 (2007).
- 34 G. Coloyan, N. D. Cultrara, A. Katre, J. Carrete, M. Heine, E. Ou, J. Kim, S. Jiang, L. Lindsay, N. Mingo, D. Broido, J. P. Heremans, J. E. Goldberger, and L. Shi, *App. Phys. Lett.* **109**, 131907 (2016).
- 35 L. J. Allen, A. J. D'Alfonso, and S. D. Findlay, *Ultramicroscopy* **151**, 11–22 (2015).
- 36 G. Henkelman, A. Arnaldsson, and H. Jónsson, *Comp. Mater. Sci.* **36**, 354–360 (2006).
- 37 R. Bistritzer, and A. H. MacDonald, *Proc. Natl. Acad. Sci. U. S. A.* **108**, 12233–12237 (2011).



We have developed a robust way of identifying small rotational disorder to help advance the understanding of twisted materials.